PalArch's Journal of Archaeology of Egypt / Egyptology

COPYRIGHT PROTECTION OF 3D ANAGLYPH COLOR IMAGE WATERMARKING OVER THIN MOBILE DEVICES

P Srikanth[1], *Adarsh Kumar*[2]

[1,2] Dept. Of Systemics, School of Computer Science, University of Petroleum and Energy Studies, Dehradun, India

P Srikanth, Adarsh Kumar Copyright Protection Of 3d Anaglyph Color Image Watermarking Over Thin Mobile Devices-- Palarch's Journal of Archaeology of Egypt/Egyptology 18(6), 15-36. ISSN 1567-214x

Keywords: Copyright Protection, Dwt, Hd, Imperceptibility, Stereoscopic, Svd, Pso, Robustness, 3d Anaglyph Image.

ABSTRACT

The exponential development in mobile devices and the internet makes the creation of digital content easier. Hence, digital content protection is essential for 3D content, especially for anaglyph images. The 3D anaglyph images are cheaper and easier to create from the stereoscopic images. Therefore, this article proposes copyright protection for 3D anaglyph color images using DWT-HD-SVD without converting the cover image into grayscale or YCbCr. Initially, the stereoscopic image consists of the left and right views that produce the different types of 3D anaglyph images. In this work, the cover image is a true and red-cyan color image, the owner's secret information as a watermark logo of color and half-color 3D anaglyph images. Then, extract the blue channel from the cover image, and applies the discrete wavelet transformation (DWT), and Hessenberg decomposition (HD) on the LL sub-band. After that, apply the Singular Value Decomposition (SVD) on the upper Hessenberg matrix. Similarly, extract the blue channel from the watermark logo and apply the SVD on the LL sub-band. Further, the embedded scaling factor ($\boldsymbol{\alpha}$) is optimized using Particle Swarm Optimization (PSO), then performs the embedded and extraction operations for various watermark sizes. The proposed approach measures the performance using MSE, PSNR, SSIM, and NCC for various attacks. Hence, the experiment results show that **10**% invisibility and **5**% robustness are enhanced over the existing approach.

INTRODUCTION

With the advancement in mobile technology, mobile devices are categorized as thin and thick devices. The thick mobile devices used to view and process the various activities on digital media. Simultaneously, the thin mobile devices only view the digital content based on the users' physical activities reflected in the virtual environment. Hence, the digital content is viewed using thin mobile devices such as Head Mounted Display (HMD) or google glass [1-3]. The

digital content over the thin mobile devices is available as 3D content. In this work, the 3D content is used as red-cyan color images such as 3D Anaglyph images. The Anaglyph images content protection is a critical problem because the users easily create the digital, and once the content is published over the internet, then owners have no control over the digital media. Hence, content protections are required for 3D Anaglyph images [4].

The digital content protection techniques are encryption/decryption, digital rights management (DRM), digital watermarking, and digital fingerprint. The encryption and decryption technique protects the data while transmitting over the network [5-7]. Once the receiver receives the data, then there is no control over the media by the content creator. Hence, encryption and decryption are not suitable for copyright protection [1, 8]. The DRM technique provides copyright protection through access control using encryption, digital signature, and watermarking. However, the digital media is distributed illegally then tracing the violent user is very difficult [1]. In Digital watermarking, the owners' secret information is embedded into the original image. This technique provides traceability for illegal copy distribution. However, this technique suffers from various robustness and imperceptibility [9-15]. The Digital fingerprint embeds the secret information as a user's identity hence provides traceability and content protection. Nevertheless, this technique suffers from a lack of transparency [16-17]. Hence, digital watermarking techniques are used to protect the 3D anaglyph images.

The existing 3D Anaglyph images copyright protection through the watermarking technique are associated with Fractional Fourier transformation (FrFT) [18-19], Discrete wavelet Transformation (DWT) [20-28], Discrete cosine Transformation (DCT) [29-30], Singular value decomposition (SVD) [29-31]. The major challenges with these techniques are

i. Suffered from robustness, imperceptibility, and computational overhead.
ii. The existing color image watermarking techniques are implemented by converting the color image into grayscale or YCbCr. Then applies the embedded and extraction operations. However, through conversion, the image information may be lost;

In this article, the 3D anaglyph color image watermarking technique is proposed using DWT, Hessenberg Decomposition (HD), and SVD. The DWT is applied by computing the decomposition level 'R' through the original image and watermark_logo length. After that, extracts the blue channel from the original image then applies the R-level DWT. Further, the HD applies on the LL sub-band and then applies the SVD on the upper Hessenberg matrix. Similarly, extract 3- channels from the watermark logo, and then apply SVD on the blue channel. Thus, the diagonal singular matrix is embedded into the original image. Further, the embedded scaling factor is optimized with the help of particle swarm optimization (PSO). After that, the red, green channels of the original image merged with the watermarked image. In the watermark extraction, extract the blue channel from the watermarked image, then applies the DWT R-level decomposition through that extract the watermark_logo then

combines the red and blue channels of the watermarked image. With this method, high robustness and invisibility are achieved against various image-processing attacks.

This article is organized: section II describes the state-of-the-art; section III and IV describe the DWT, HD, SVD, and PSO and proposed watermark technique. Section V explains experimental results and analysis. Finally, describes the conclusion in Section VI.

STATE OF THE ART

The existing watermarking techniques for 3D anaglyph images are in the frequency domain. In this, the owners' secret information is incorporated into the original image spectrum. Hence, this technique provides good robustness but minimizes the quality of the images. The current study explores the different 3D anaglyph image watermark techniques implemented by various researchers.

Bhatnagar et al. [19] method for the 3D anaglyph image watermarking using Fractional Fourier Transformation for color channels embedded with SVD. The color channels are obtained through reversible integer transformation on RGB. This technique provides high robustness and imperceptibility. However, this method is not used any embedded watermarking approach; hence any users can claim ownership rights on digital media.

Deng et al. [32] proposed a 3D model watermarking with the affine transformation invariance through Nelson norm and the watermark embedded into the grayscale image. This approach resists the affine transformation and Gaussian noise attack, but poor resist for the other attacks.

Ivy et al. [33] 3D anaglyph image watermarking scheme uses the 3D-DWT and Jacket matrix. The 3D-DWT is applied to the cover image and the jacket matrix is applied by selecting the middle sub-band. After that, in each diagonal block, the watermark is embedded. Hence, this approach provides robustness for geometric and signal attacks. However, this will incur computation overhead.

Ruchika et al. [30] uses the DWT approach and applies on the right image of the cover image and, and watermark_logo then performs the embedding operation. After that, combines the left image and watermarked image that produces the watermarked anaglyph 3D image. This approach computationally slow because of the right image reconstruction.

David et al. [34] method for color image watermarking through the DCT, dither modulation (DM), and quantization index modulation (QIM). In embedded operation, the cover and watermark RGB images are converted into YCbCr. The cover image's luminance 'L' is selected and divides into the 8x8 blocks, then applies the DCT. After that, the QIM-DM algorithm modifies the first 12 bits of the DCT. Similarly, the watermark image's luminance is selected, then applies the subsampling (4:2:0) that obtains the watermark, then applies the QIM-DM performs the insertion per block. This approach provides

robustness and imperceptibility but creates the computational overhead based on the image size.

Devi et al. [35] approach uses different techniques as DWT, Advanced Encryption Standards (AES), and Genetic Algorithm (GA). This approach uses the Middlebury stereo dataset that consists of the red-cyan 3D anaglyph images as cover images then apply the DWT. After that, the DWT bits are optimized using GA and fed into the Back Propagation Network (BPN). The AES algorithm is applying to the watermark logo then performs the embedded operation using optimized bits that provide high robustness. Nevertheless, the training phase creates the computational overhead and the training phase is failed then no recovery mechanism available.

Devi et al. [4] proposed copyright protection for 3D anaglyph images uses DWT and SVD. This method extracts the blue channel from an anaglyph image then applies it to the DWT. The vertical level co-efficient is selected, then applies the Fast wavelet Hadamard Transformation and applies the SVD. After that, scramble the watermark logo into 32x32 size by using Arnold Transformation and then apply the embedded operation based on the scaling factor. This approach provides robustness and imperceptibility for the watermark logo size is 32x32. However, this approach provides poor resistance against filtering and rotation attacks.

Subhadeep Koley [31] method uses the lifting wavelet transformation (LWT) and tensor-SVD (T-SVD) for 3D anaglyph images. The LWT is applying on the 3D anaglyph image through that select the LL sub-band then applies the T-SVD. After that, scramble the watermark logo using Arnold's cat map (ACM) then apply the embedded processing that generates the watermarked image. This approach provides robustness and imperceptibility.

Critical Analysis: from the existing study, it has been observed that the major challenges

i. The copyright protection for color images done through the conversion of RGB into Grayscale or YCbCr images, then applied the embed operation. Which produces the information lost?
ii. Most of the existing work focused on DWT and SVD.
iii. The invisibility and robustness still need to be enhanced.
iv. None of the techniques is focused on the variable watermark logo sizes for copyright protection.

PRELIMINARIES

This section describes the four technologies as DWT, HD, SVD, and PSO are used in the copyright protection of 3D anaglyph color images. In the frequency domain, the most widely used watermark technique is DWT that improves the watermarking performance against various robustness attacks, and to enhance the robustness further, the HD is used. However, the DWT technique suffers from geometric attacks, which are managed by the decomposition techniques such as SVD is used, and it handles the false positive problem. Finally, the embedded strength of the watermark varies from

image to image. Hence, the embedded strength is optimized using nature-inspired algorithms such as PSO.

Discrete Wavelet Transformation (Dwt)

DWT is the most widely used mathematical formalization, which decomposes the image into a series of sub-band coefficients as an approximation (LL), vertical (LH), horizontal (HL), and detail (HH). This decomposition is applying recurrently that satisfies the watermark requirement sub-bands size. The coefficients are obtained using the Haar filter as follows [36]

$$LL(i,j) = \frac{CI(i,j) + CI(i,j+1) + CI(i+1,j) + CI(i+1,j+1)}{2} \quad (1)$$

$$LH(i,j) = \frac{CI(i,j) + CI(i,j+1) - CI(i+1,j) - CI(i+1,j+1)}{2} \quad (2)$$

$$HL(i,j) = \frac{CI(i,j) - CI(i,j+1) + CI(i+1,j) - CI(i+1,j+1)}{2} \quad (3)$$

$$HH(i,j) = \frac{CI(i,j) - CI(i,j+1) - CI(i+1,j) + CI(i+1,j+1)}{2} \quad (4)$$

Here, $CI, i\ and$ j denotes the image and its coordinates. The image's most important information is available in the LL sub-band. Hence, the robustness of watermarking is obtained through the LL sub-band compared to other sub-bands [37-38].

Hessenberg Decomposition (Hd)

HD is a square matrix, which decomposes the matrix "A" into factorization as follows [39-41].

$$QHQ^T = HD(A) \quad (5)$$

Where Q and H denote the orthogonal and upper Hessenberg matrix, the upper Hessenberg matrix means the below the first diagonal of the primary diagonal consist of the zero's, i.e., $h_{ij} = 0\ where\ i > j + 1$. The HD computes the Householder matrix (P), which is represented as

$$P = \frac{I_n - 2\mu\mu^T}{\mu^{T\mu}} \quad (6)$$

$$H = (p_1, p_2, \ldots\ldots\ldots p_{n-2})^T A(p_1, p_2 \ldots\ldots\ldots\ldots p_{n-2}) \quad (7)$$

Here I_n denotes the identity matrix with size $n \times n$, μ is non-zero vector and Q=$(p_1, p_2 \ldots\ldots\ldots\ldots p_{n-2})$. Hence, from equation 7, the simplified equations are produced as 8 and 9 as

$$H = Q^T A\, Q \tag{8}$$

$$A = QHQ^T \tag{9}$$

Let us assume an image's size is 4×4then the pixel values are in the matrix 'A.'

$$A = \begin{bmatrix} 134 & 154 & 142 & 123 \\ 119 & 157 & 157 & 138 \\ 119 & 123 & 142 & 147 \\ 131 & 146 & 138 & 138 \end{bmatrix} \tag{10}$$

After applying the HD decomposition on 'A,' the resultant orthogonal matrix Q and upper Hessenberg matrix H are as follows

$$Q = \begin{bmatrix} 1 & 0 & 0 & 0 \\ 0 & 0.3744 & -0.2086 & -0.4093 \\ 0 & -0.3744 & -0.2162 & 0.4049 \\ 0 & -0.3833 & 0.4123 & 0.0023 \end{bmatrix} \tag{11}$$

And

$$H = \begin{bmatrix} 134.000 & -249.0750 & -12.2510 & -4.4043 \\ -220.5952 & 302.5262 & 0.3495 & -12.3245 \\ 0 & 20.3807 & 3.5942 & -1.3683 \\ 0 & 0 & 8.3508 & 3.3496 \end{bmatrix} \tag{12}$$

Subsequently from RGB images extract the R, G, and B channels and the pixel values are range from 0 to 255, and neighboring pixel values are not changing because of the small block size. Hence, the desired orthogonal unitary matrix "Q" has smaller difference values as$0.3744, -0.3744, -0.3833$. Therefore, the smaller modification in the embedded process will improve the imperceptibility, and the HD approach takes less time than other decomposition techniques [42].

Singular Value Decomposition (Svd)

The SVD is the symmetric matrix factorization divided into the three singular matrix components such as U, S, V are computed from matrix 'A' as

$$U, S, V = SVD(A) \tag{13}$$

The U, S, V denotes the left, diagonal, and right singular matrix with positive real values of 'n' Eigenvalues [43-45]. Let us assume 'A' is a rectangle matrix with $m \times n$ size then the generated singular matrices sizes after applying the SVD areU_{mm}, S_{mn}, V_{nn}. Hence, the representation of'S is as follows

$$S = \begin{bmatrix} \sigma_1 & 0 & 0 & \dots. & 0 \\ 0 & \sigma_2 & 0 & \dots. & 0 \\ 0 & 0 & \sigma_3 & \dots. & 0 \\ 0 & 0 & 0 & \dots. & 0 \\ 0 & 0 & 0 & \dots. & \sigma_n \end{bmatrix} \quad (14)$$

Here $U_{mm}\ and\ V_{nn}$ are orthogonal eigenvector of matrix AA^T andA^TA.

Particle Swarm Optimization (Pso)

The nature-inspired algorithm finds the optimum solution based on the population size. In this work, the PSO algorithm finds the feasible solution regards the bird in the search domain for the optimized problem as a particle [46-47]. Every particle has the velocity that controls the birds flying distance and direction Moreover; optimization is governing by using a fitness function.

In PSO, each particle knows its global best values, the best position, and solution. Hence, in each iteration the particles change their speed, find the local and global best solution as Pbest and Gbest [48-49]. The Pbest determines the particles' own flying experiences, compared with their fellow particles flying experience that determines the Gbest as the highest value among all the Pbest. The particles change their positions between the current position with the Pbest position and the current position with the Gbest position. Hence, determines the best position of the individual particle and global best position in the search space as Pbseti= (pbesti1, pbesti2…. pbestin) and Gbesti= (Gbest1, Gbest2 …Gbestn) among the Pbesti. Hence, updates the velocity and positions are as follows

$$V_{k+1}^n = W * V_k^n + C_1 * r_1 * (Pbest_k - X_k^n) + c_2 * r_2 * (Gbest_k - X_k^n) \quad (15)$$

$$X_{k+1} = X_k + V_{k+1} \quad (16)$$

Here, n denotes the population size, $c_1 and\ c_2$ are acceleration factors, W inertia weight, $r_1 and\ r_2$ specifies the random numbers that are normalized to [0,1]. $V_k^n\ and\ X_k^n$ Indicates the velocity and position of the particle; k is the iteration.

Proposed Color Image Watermarking Method

The 3D anaglyph color image watermarking approach is fabricated from the stereoscopic image. The stereoscopic image consists of the two images as the left and right eye view. Extract the red channel from the left image, and extract the green and blue channels from the right image. After that, generates the cyan color image by combining the green and blue channels. Hence, construct the 3D anaglyph image as a red-cyan color image as shown in Fig.1.

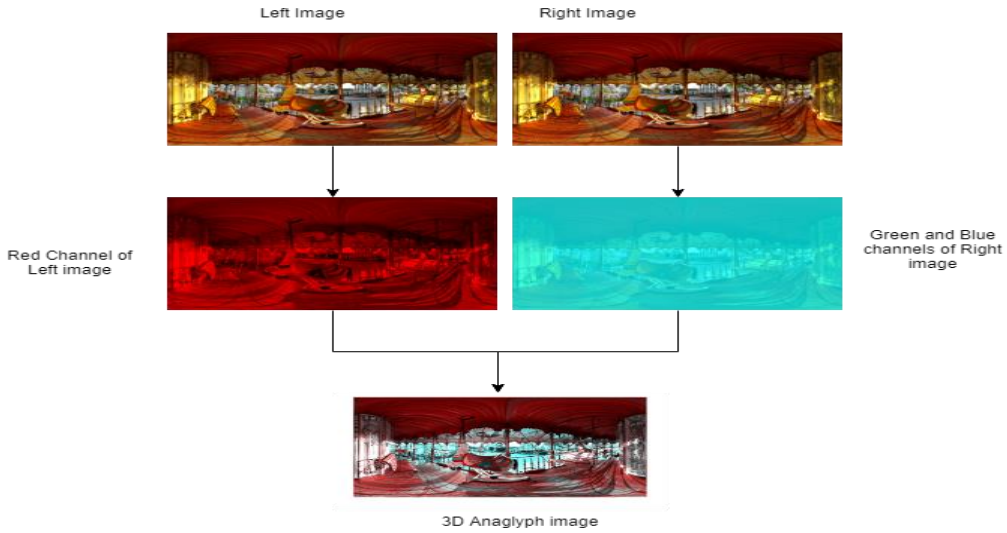

Fig.1 3D Anaglyph Red-Cyan Image Construction

The 3D anaglyph color images represented as true, mono, color, half-color, and optimized-color. In this work, the original image is a true anaglyph, and owners' secret information as watermark logo is a Color anaglyph image. The construction of true and color anaglyph images shown in equations 17 and 18.

$$True\ Anaglyph = \begin{bmatrix} 0.299 & 0.587 & 0.114 \\ 0 & 0 & 0 \\ 0 & 0 & 0 \end{bmatrix} \begin{bmatrix} r_i \\ g_i \\ b_i \end{bmatrix} + \begin{bmatrix} 0 & 0 & 0 \\ 0 & 0 & 0 \\ 0.299 & 0.587 & 0.114 \end{bmatrix} \begin{bmatrix} r_j \\ g_j \\ b_j \end{bmatrix} \quad (17)$$

$$Color\ Anaglyph = \begin{bmatrix} 1 & 0 & 0 \\ 0 & 0 & 0 \\ 0 & 0 & 0 \end{bmatrix} \begin{bmatrix} r_i \\ g_i \\ b_i \end{bmatrix} + \begin{bmatrix} 0 & 0 & 0 \\ 0 & 1 & 0 \\ 0 & 0 & 1 \end{bmatrix} \begin{bmatrix} r_j \\ g_j \\ b_j \end{bmatrix} \quad (18)$$

Initially, extract the B-channel from the cover image (True anaglyph), and watermark logo (color anaglyph) image and then, perform the embedded process. The proposed watermark-embedding algorithm consists of three levels as (i) Pre-Process (ii) Watermark-embedding (iii) Post-Process.

WATERMARK EMBEDDING ALGORITHM

The cover image denotes the 3D True Anaglyph image with 512×512 size and watermark logo as the 3D Color Anaglyph image with 256×256 size. The watermark-embedded process is performing the various decomposition on the cover image as DWT, HD, and SVD. Hence, the watermark embedding process as follows.

Pre-Processing

Step1: The cover image (CI_{RGB}) and watermark_logo image (WI_{RGB}) are RGB color images, from that images extract the R, G, B channels as CI_r, CI_g, CI_b andWI_r, WI_g, WI_b. The blue channel (CI_b) of the cover image is selected because the blue channel is less intense to human eyes.

$$CI_r = CI_{RGB}(:,:,1) \quad CI_g = CI_{RGB}(:,:,2) \quad CI_b = CI_{RGB}(:,:,3) \tag{19}$$

$$WI_r = WI_{RGB}(:,:,1) \quad WI_g = WI_{RGB}(:,:,2) \quad WI_b = WI_{RGB}(:,:,3) \tag{20}$$

Step2: The length of the CI_{RGB} and WI_{RGB} are computed, based on that evaluates the level of decomposition as

$$M = length(CI_{RGB}) \qquad N = length(WI_{RGB}) \qquad R = \log_2\left(\frac{M}{N}\right) \tag{21}$$

Step3: The blue channel of the cover image (CI_b) is decomposed to R-levels through the DWT with Haar Transformation. Hence, it acquires the different sub-bands as$[LL, HL, LH, HH]$. Further, the HD decomposition applied on LL-sub-band through that obtains the upper Hessenberg matrix.

$$[LL, HL, LH, HH] = DWT(CI_b, 'haar') \tag{22}$$

$$[P, H] = hess(LL) \tag{23}$$

Step4: compute the size of the upper Hessenberg matrix (H) and resize the WI_r, WI_g, WI_b to the size of H. then apply the SVD decomposition on H andWI_b.

$$[U_c, S_c, V_c] = SVD(H) \tag{24}$$

$$[U_w, S_w, V_w] = SVD(WI_b) \tag{25}$$

Embedding Process

Step5: After applying the SVD on H and WI_b, selects the diagonal singular matrix as S_c andS_w. Then computes the watermark diagonal singular value.

$$Cw_{hat} = S_c + (\alpha * S_w) \tag{26}$$

Where Cw_{hat} specifies the watermark singular value and α is embedded scaling factor which manages the robustness and imperceptibility tradeoffs.

Post-Processing

Step6: in post-processing, apply the inverse of SVD that to obtains the watermark sub-band by equation 27. After that apply the inverse of HD that generates the lower sub-band frequency which is defined in equation 28.

$$C_{hat} = U_c * Cw_{hat} * V_c' \quad (27)$$

$$LL_{hat} = P * C_{hat} * P' \quad (28)$$

Step7: Apply the inverse DWT (IDWT) based on the R-level using LL_{hat} as a lower sub-band through that generate the watermarked_image.

$$watermarked\ image = idwt(LL_{hat}, HL, LH, HH) \quad (29)$$

Step8: combine the R, G channels with the watermarked image that produces the RGB watermarked image.

WATERMARK EXTRACTION ALGORITHM

In the extraction process, the owners' secret information is obtained as a watermark logo from the cover image. The extraction process consists of three levels as (i) Pre-Process (ii) extraction (iii) Post-Process.

Pre-Processing for Extraction

Step9: Extract the R, G, B channels from the attacked image (watermarked image) named as $MI_r, MI_g, and\ MI_b$.The MI_b is used for the watermark extraction.

$$MI_r = watermarked\ image(:,:,1)$$

$$MI_g = watermarked\ image(:,:,2)$$

$$MI_b = watermarked\ image(:,:,3) \quad (30)$$

Step10: Apply the R-level DWT on MI_b and HD on LL_w which are defined in equations 31 and 32.

$$[LL_w, HL_w, LH_w, HH_w] = dwt(MI_b) \quad (31)$$

$$C_w = hess(LL_W) \quad (32)$$

Step11: Apply the SVD on the upper Hessenberg matrix of the watermarked image defined in equation 33.

$$[Uw_{hat}, Sw_{hat}, Vw_{hat}] = SVD(C_w) \quad (33)$$

Watermark Extraction

Step12: The watermark is extracted by subtracting the$Sw_{hat} and\ S_w$, which are obtained from the step11 and step4. After that, the result is divisible by the embedded scaling factor(α). Hence, the singular diagonal matrix produces using equation 34.

$$Swb_{hat} = \frac{Sw_{hat} - Sw}{\alpha} \quad (34)$$

Post-Processing for Watermark Extraction

Step13: Apply the inverse SVD to extract the watermarked image MI_{hat} using equation 35.

$$MI_{hat} = U_w * Swb_{hat} * V_w' \qquad (35)$$

Step14: combine the results of $MI_r, MI_g and\ MI_{hat}$ values, which are obtained in steps 9 and 13 through that produces the extracted watermarked image.

Scaling Factor Optimization with Pso

In digital watermark, the invisibility and robustness depend on the embedded strength such as(α). The small changes in the scaling factor will result in changes in robustness and imperceptibility. Hence, the selection of scaling factor is the critical activity in the watermarking process because the large scaling factor provides high robustness but degrades the quality. The scaling factor varies from image to image; hence, the manual selection of the scaling factor is a time-consuming process. Therefore, optimized techniques are required to search for the best-optimized solution to provide robustness and invisibility. The proposed optimization technique provides the automatic scaling factor that embeds the watermark into the original image. Hence, in each iteration different attacks are applying through that analyzes the optimum embedded scaling factor. The optimization process starts from the selection of parameters such as the population size, the number of iterations, inertia, acceleration factors, initial position, and velocity are present in Table 1 and the process flow in Fig.2. The particles move in the search space to finds the optimum fitness value, updates the velocity and position. The fitness value evaluated as

$$fitness = \frac{n}{(PSNR + \sum_{i=1}^{n} NCC_i)} \qquad (36)$$

Where PSNR value is assessed between the original and watermarked image, NCC value is calculated between the watermark logo and extracted watermark for each attack, 'n' denotes the number of operations.

Table1: List of Parameters Used for PSO Watermarking

Parameter name	value
Population size	50
iterations	100
inertia	1.0
acceleration factors	$C_1 = 2, C_2 = 2$

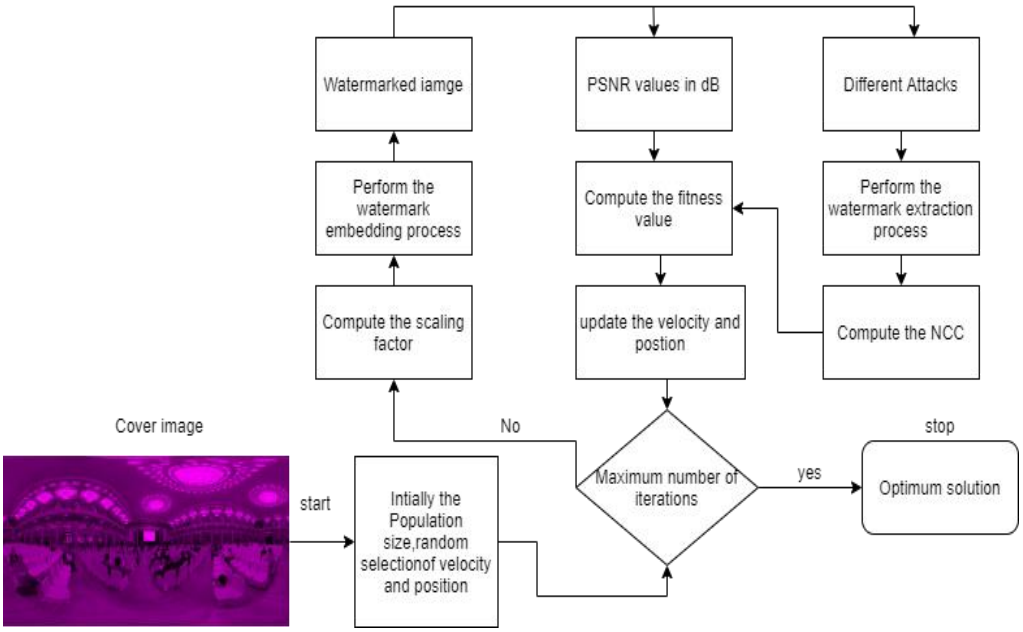

Fig.2 Pso Process Flow Diagram

EXPERIMENTAL RESULTS AND PERFORMANCE ANALYSIS

The performance of the proposed watermarking scheme on 3D anaglyph images without converting the RGB image into grayscale or YCbCr. This approach measures the invisibility, robustness, and embedded payload. This approach is implemented on the laptop with a Core i3-7100U CPU @ 2.40GHz, 4GB memory, Windows Operating System with 64-bit, and MATLAB R2016a (64-bit version).

Experimental Setup

The proposed algorithm is evaluated using the 2D salient images converted into different type's 3D Anaglyph images such as Red-Cyan, True, Mono, Color, Half-Color, and Optimized-Color and the same images are used for watermark logos. These images sizes are for the cover image as $512 \times 512 \times 3$ and multiple sizes of watermark logos such as $256 \times 256 \times 3$,$128 \times 128 \times 3$ and $64 \times 64 \times 3$. The 3D anaglyph images are depicted in Fig.3.

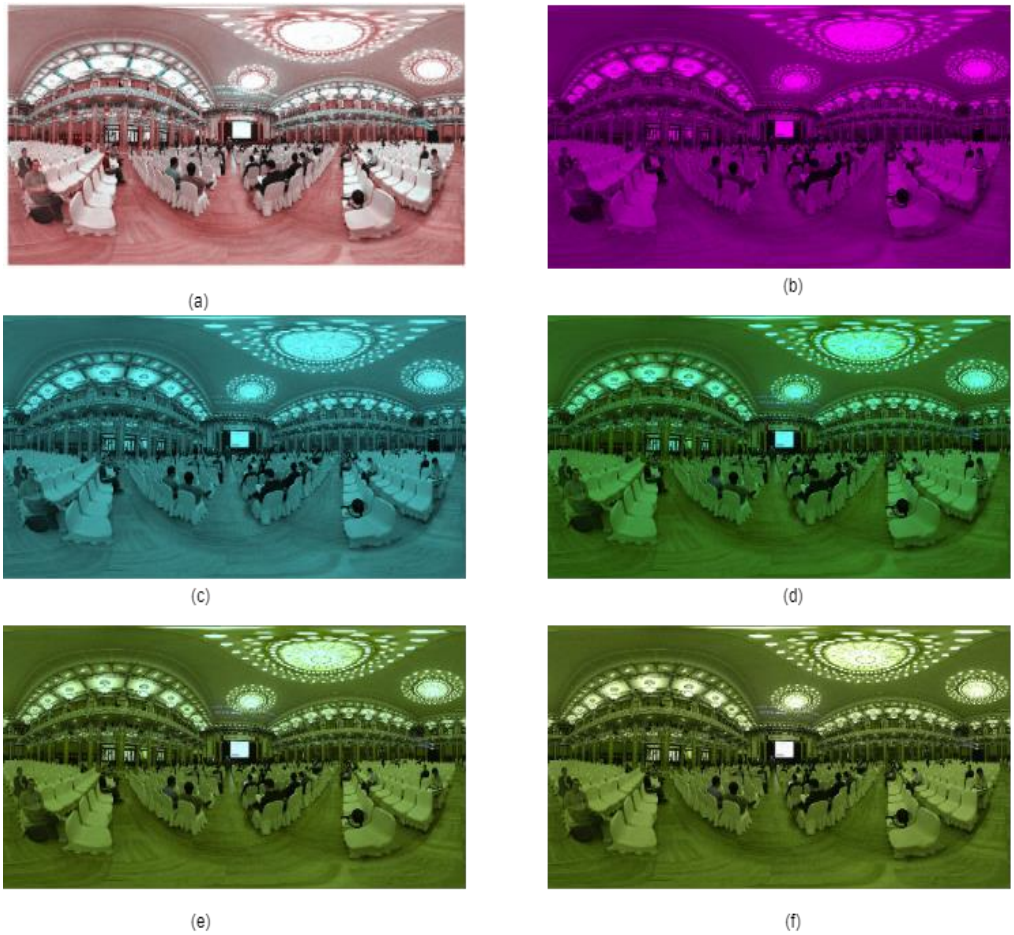

Fig.3 3D Anaglyph Images: (a) red-cyan (b) True (c) Mono (d) Color (e) Half-Color (f) Optimized Color

Performance Metrics

The proposed approach performance is analyzed using MSE, PSNR, SSIM, MSE, and NCC. The PSNR, MSE, and SSIM are used to assess the image quality and NCC is used for the image robustness. The mathematical formulas as follows

$$MSE = 1/(M * N) \sum_{x=1}^{M} \sum_{y=1}^{N} [CI(x,y) - MI(x,y)] \quad (37)$$

$$(PSNR)_{dB} = 10 \log_{10}({CI^2}_{max} /MSE) \quad (38)$$

$$SSIM(CI, MI) = \frac{(\mu_{CI}\mu_{MI}+d_1)}{({\mu^2}_{CI}+{\mu^2}_{MI}+d_1)} * \frac{(\sigma_{CIMI}+d_2)}{({\sigma^2}_{CI}+{\sigma^2}_{MI}+d_2)} \quad (39)$$

Where CI, MI denotes the cover image and watermark image, x, y are their coordinates. The lower value for MSE denotes the high quality. The PSNR value is evaluated based on the MSE hence the PSNR is higher than the high

quality. The structural similarity specifies the invisibility capability of the image which lies in between [0,1] and the value nearer to 1 means a similar image. From equation 39, $\mu_{CI,}\mu_{MI}$ denotes the mean of CI and MI. ${\sigma^2}_{CI}, {\sigma^2}_{MI}$, and σ_{CIMI} are variance and covariance of CI and MI. $d1 and\ d2$ signifies the weak denominators. Besides, the robustness of the proposed approach is assessed using NCC. The mathematical formula for NCC is measured between watermark logo (WI) and extracted watermark (MI_{hat}). The robustness value lies in between [0, 1], and the value closer to 1 means highly robust.

$$NC = \frac{\left(\sum_{x=1}\ \sum_{y=1} WI(x,y)\, MI_{hat}(x,y)\right)}{\sqrt{\sum_{x}\ \sum_{y}[WI(x,y)]^2}\ \sqrt{\sum_{x}\ \sum_{y}[MI_{hat}(x,y)]^2}} \quad (40)$$

EXPERIMENTAL RESULTS

The proposed color image watermarking schema performance is evaluated in the phases such as invisibility and robustness under different attacks. After that, the PSO optimization embedded strengths are used to assess the image quality.

Invisibility

The invisibility evaluation depends on the watermark embedding approach; in this, the cover image is embedded with a watermark logo using the embedded scaling factor. To validate the quality of the image using Fig.3 (a-c) as a cover image and Fig. 3(d-e) as a watermark logo. Hence, the watermarked images depict in Fig.4 (a-c) and Fig. 5(a-c), the extracted watermark images depict in Fig.4 (d-f) and Fig.5 (d-f).

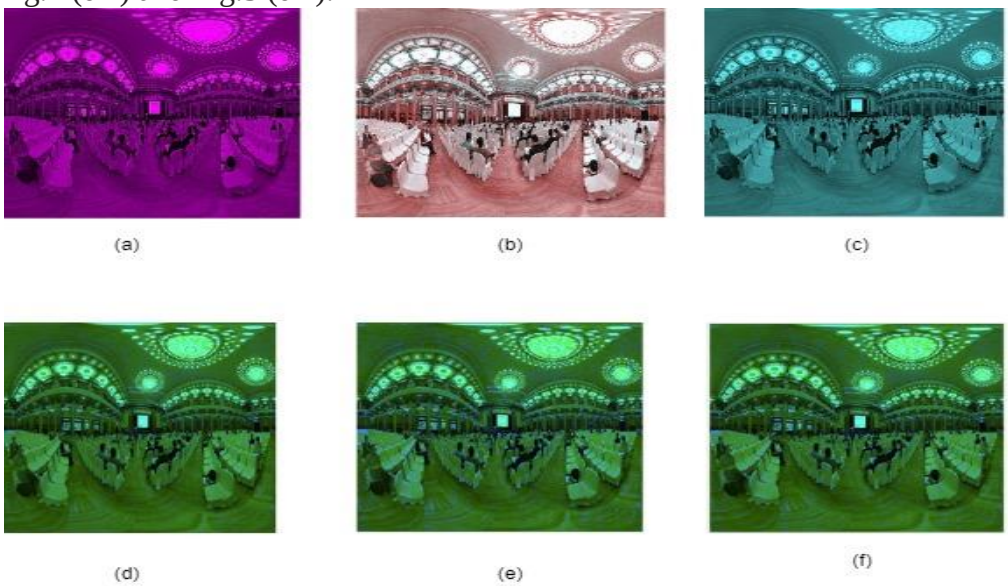

Fig.4 (a) watermarked true 3D Anaglyph image, (b) watermarked red-cyan 3D anaglyph image, (c) watermarked mono 3D anaglyph image (d) color 3D anaglyph extracted watermarked image from (a), (e) color 3D anaglyph extracted watermarked image from (b), (f) color 3D anaglyph extracted watermarked image from (c)

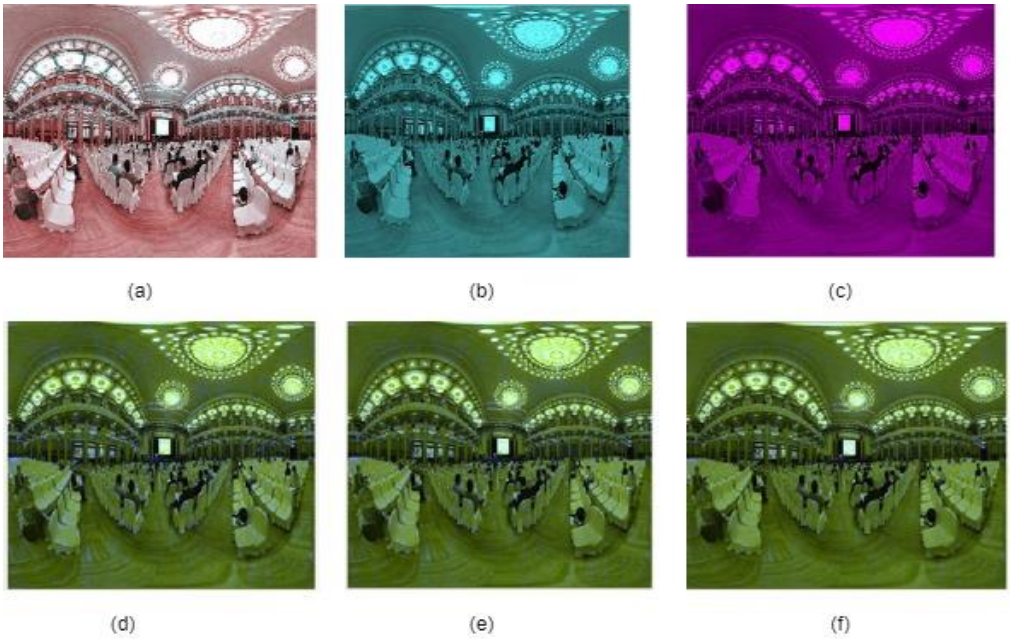

Fig.5 (a) watermarked red-cyan 3D Anaglyph image, (b) watermarked mono 3D anaglyph image, (c) watermarked true 3D anaglyph image (d) halfcolor 3D anaglyph extracted watermarked image from (a) ,(e) halfcolor 3D anaglyph extracted watermarked image from (b), (f) halfcolor 3D anaglyph extracted watermarked image from (c).

The proposed approach performance is assessed using MSE, PSNR, SSIM, and NCC are listed in Table 2. In Table2, the secret information is embedded into the cover image thus watermark logos have taken as color and half color 3D anaglyph images with different sizes. Based on the experimental results the PSNR values are more than 45dB, SSIM value is 1, and MSE value lesser than 70 produces good invisibility and shows the robust performance through the proposed approach.

Table 2: The Proposed Approach's Performance Analysis

Cover image	**Watermark logo**	**Watermark logo size**	**MSE**	**PSNR (dB)**	**SSIM**	**NCC**
True Anaglyph	Half-color Anaglyph	256x256	0.69682	49.62	0.9999	1
True Anaglyph	Half-color Anaglyph	128x128	0.21381	54.7867	0.9999	1
True Anaglyph	Half-color Anaglyph	64x64	0.039146	62.2039	1	1
Mono Anaglyph	Half-color Anaglyph	256x256	0.6871	49.6811	0.99982	1
Mono Anaglyph	Half-color Anaglyph	128x128	0.21253	54.8135	0.99994	1
Mono Anaglyph	Half-color Anaglyph	64x64	0.039145	62.204	0.99999	1

Red-Cyan Anaglyph	Half-color Anaglyph	256x256	0.67157	49.7703	0.9992	1
Red-Cyan Anaglyph	Half-color Anaglyph	128x128	0.19136	55.2751	0.9997	1
Red-Cyan Anaglyph	Half-color Anaglyph	64x64	0.046205	61.4839	0.9999	1
True Anaglyph	Color Anaglyph	256x256	0.69479	49.6321	0.9999	1
True Anaglyph	Color Anaglyph	128x128	0.21307	54.8012	0.9999	1
True Anaglyph	Color Anaglyph	64x64	0.038914	62.2298	1	1
Mono Anaglyph	Color Anaglyph	256x256	0.68531	49.6918	0.99982	1
Mono Anaglyph	Color Anaglyph	128x128	0.21176	54.8287	0.99994	1
Mono Anaglyph	Color Anaglyph	64x64	0.039145	62.204	0.99999	1
Red-Cyan Anaglyph	Color Anaglyph	256x256	0.66959	49.782	0.99921	1
Red-Cyan Anaglyph	Color Anaglyph	128x128	0.19051	55.2935	0.99973	1
Red-Cyan Anaglyph	Color Anaglyph	64x64	0.046205	61.4839	0.9999	1

The proposed approach also uses nature-inspired optimized algorithms that optimize the embedded strength. Hence, the performance results for the cover image: true anaglyph and red-cyan anaglyph images with watermark logo as color anaglyph then the embedded strength varies between [0.005, 0.1]. Thus, the obtained results are depicted in Table 3.

Table 3: Performance Analysis Under Different Scaling Factors

	True Anaglyph image				**red-cyan Anaglyph image**			
SF	**MSE**	**PSNR (dB)**	**SSIM**	**NC**	**MSE**	**PSNR (dB)**	**SSIM**	**NC**
0.005	0.000181	85.56453	1	1	0	84.6453	1	1
0.01	0.026471	63.90303	0.999998	1	0.036691	62.4852	0.999916	1
0.015	0.064301	60.04866	0.999994	1	0.078403	59.18745	0.999885	1
0.02	0.15192	56.31464	0.999978	1	0.124204	57.18945	0.999855	1
0.025	0.224443	54.61975	0.999966	1	0.211185	54.88416	0.999714	1
0.03	0.3021	53.3293	0.999955	1	0.295849	53.4201	0.999624	1
0.035	0.403793	52.06921	0.999944	1	0.368945	52.46119	0.999561	1
0.04	0.483645	51.28554	0.999934	1	0.46563	51.4504	0.999439	1
0.045	0.5846	50.46222	0.999922	1	0.574118	50.54079	0.999304	1
0.05	0.707729	49.63213	0.999904	1	0.683718	49.78203	0.999206	1
0.055	0.857615	48.79788	0.999882	1	0.819635	48.9946	0.99906	1
0.06	1.023675	48.02918	0.999857	1	0.973361	48.24807	0.998875	1
0.065	1.179187	47.41498	0.999836	1	1.115234	47.65714	0.998754	1

0.07	1.355488	46.80985	0.999815	1	1.279391	47.06077	0.998592	1
0.075	1.533609	46.27366	0.999793	1	1.4631	46.47806	0.998372	1
0.08	1.729097	45.75261	0.999767	1	1.646614	45.96489	0.998188	1
0.085	1.94732	45.23643	0.999736	1	1.83801	45.48732	0.998019	1
0.09	2.176038	44.75414	0.999703	1	2.054223	45.00433	0.997788	1
0.095	2.413799	44.30379	0.999669	1	2.271529	44.56762	0.997567	1
0.1	2.653086	43.89329	0.999634	1	2.491845	44.16559	0.997363	1

Based on Table 3, the performance of PSO optimization obtains the better imperceptibility results are acceptable for different embedded scaling factor values achieved for MSE, PSNR, and SSIM. The robustness is also acceptable as per the results shown in Table 3. Hence the proposed method requires less computational power and lossless watermark image restoration.

Robustness

The proposed scheme evaluates the robustness under different attacks that destroyed the secret information, which is embedded as a watermark. Hence, the proposed approach robustness validated against the various geometric, signal, and temporal attacks. The results are shown in Fig.6 with different watermark logo sizes.

Table 4: Robustness for Different Watermark Sizes

	True Anaglyph image			**red-cyan Anaglyph image**		
	256x256	128x128	64x64	256x256	128x128	64x64
MSE	0.69479	0.21307	0.03891	0.66959	0.19051	0.04621
PSNR (dB)	49.6321	54.801	62.2298	49.782	55.2935	61.4839
SSIM	0.99999	0.99997	1	0.99921	0.99973	0.9999
NC	1	1	1	1	1	1

Based on Table 4, the robustness and invisibility are analyzed under different watermark sizes. Hence, the robustness of the proposed watermark algorithm is explored under different parameter values with several attacks then the results are shown in Table 5.

Table 5: Robustness for Different Attacks

	Parameters	**True anaglyph image**		**red-cyan anaglyph image**	
Attacks		**NC**	**SSIM**	**NC**	**SSIM**
'No Attacks'	0	1	0.99997	1	0.99973
'Gaussian low-pass filter'	3x3	1	0.97877	1	0.88577
'Median'	3x3	1	0.98267	1	0.90748
'Gaussian noise'	0.001	1	0.98529	1	0.94048

'Salt and pepper noise'	0	1	0.99585	1	0.98587
'Rotating attack'	2 degree	1	0.8402	1	0.47614
'JPEG compression'	50	1	0.96827	1	0.94474
'JPEG2000 compression'	12	1	0.99274	1	0.98029
'Sharpening attack'	0.8	1	0.99253	1	0.96478
'Average filter'	0	1	0.99274	1	0.88221
'Motion blur'	0	1	0.99253	1	0.79829

Based on Table 5 results the proposed watermarking approach provides the robustness for geometric, signal, and temporal attacks on watermark images. The performance of the proposed scheme with the existing approach is depicted in Table 6. Hence, the results show that the proposed scheme provides better invisibility compare to the existing approach.

Table 6: Comparison Between Proposed and Existing Method

			Proposed Approach			Method [26]		
Cover image	Watermark logo	Watermark logo size	**MSE**	**PSNR (dB)**	**SSIM**	MSE	PSNR (dB)	SSIM
Red-cyan Anaglyph	Color Anaglyph	256x256	**0.66959**	**49.782**	**0.9992**	1.784	41.7009	0.9949
Red-cyan Anaglyph	Color Anaglyph	128x128	**0.19051**	**55.2935**	**0.9997**	1.6185	41.9799	0.9954
Red-cyan Anaglyph	Color Anaglyph	64x64	**0.04620**	**61.4839**	**0.9999**	1.4763	42.3733	0.9965

The invisibility of the proposed method is evaluated under different attacks with the comparison of the existing approach then the results are shown in Table 7.

	Proposed approach		**Method [26]**	
Attacks	**PSNR (dB)**	**SSIM**	**PSNR (dB)**	**SSIM**
'No Attack'	**55.2935**	**0.99973**	41.9799	0.99545
'Gaussian low-pass filter'	**24.514**	**0.88577**	24.468	0.88312
'Median'	**25.4177**	**0.90748**	25.3603	0.90439
'Gaussian noise'	**30.1178**	**0.94048**	29.8585	0.93724
'Salt and pepper noise'	**34.8849**	**0.98587**	34.3802	0.98174
'Rotating attack'	**13.9194**	**0.47614**	13.9168	0.47343
'JPEG compression'	**28.5172**	**0.94474**	28.4037	0.94284

'JPEG2000 compression'	**34.4887**	**0.98029**	34.0454	0.97842
'Sharpening attack'	**27.4927**	**0.96478**	27.3298	0.9606
Histogram equalization'	**16.993**	**0.61539**	16.9723	0.61196
'Average filter'	**24.3845**	**0.88221**	24.3394	0.87958
'Motion blur'	**21.7215**	**0.79829**	21.7023	0.79636

The performance of the proposed approach produces better invisibility and robustness for different attacks with the comparison of the existing method.

CONCLUSION

The robust anaglyph image watermarking approach uses the RGB color images as a cover and watermark images that provide imperceptibility and robustness. In this work, DWT-HD-SVD transformations are used along with PSO optimization through optimizes the embedded scaling factor. The experimental results of the proposed approach depict the embed watermark technique provides high robustness and invisibility with MSE, PSNR, SSIM, and NCC. Besides, the proposed method evaluates the robustness and invisibility for variable sizes of the watermark logos through that it achieves better performance results for the various attacks. In the future, the proposed approach further enhances to resist the rotation and histogram attacks.

REFERENCES

Qureshi, A., Rifa-Pous, H., & Megias, D. (2016). State-of-the-art, challenges and open issues in integrating security and privacy in P2P content distribution systems. *2016 Eleventh International Conference on Digital Information Management (ICDIM)*.

Krishnamurthi, R., Gopinathan, D., & Kumar, A. (2021). Wearable Devices and COVID-19: State of the Art, Framework, and Challenges. *Studies in Systems, Decision and Control Emerging Technologies for Battling Covid-19*, 157-180.

Singhal, R., Kumar, A., Singh, H., Fuller, S., & Gill, S. S. (2020). Digital device-based active learning approach using virtual community classroom during the COVID-19 pandemic. *Computer Applications in Engineering Education*.

Devi, H. S., & Singh, K. M. (2020). Red-cyan anaglyph image watermarking using DWT, Hadamard transform, and singular value decomposition for copyright protection. *Journal of Information Security and Applications, 50*, 102424.

Kumar, A., Aggarwal, A., Sharma, K., & Goyal, M. (2021). Active learning in E-learning: A case study to teach elliptic curve cryptosystem, its fast computational algorithms and authentication protocols for resource constraint RFID-sensor integrated mobile devices. E-learning Methodologies: Fundamentals, Technologies and Applications, 285-317.

Kumar, A., & Sharma, D. K. (2020). Survey and Analysis of Lightweight Authentication Mechanisms. Cryptography - Recent Advances and Future Developments.

Kumar, A., Gopal, Krishna., & Aggarwal, A. (2016). Design and analysis of lightweight trust mechanism for secret data using lightweight cryptographic primitives in MANETs. 18. 1-18.

Zadokar, S. R., Raskar, V. B., & Shinde, S. V. (2013). A digital watermarking for anaglyph 3D images. *2013 International Conference on Advances in Computing, Communications and Informatics (ICACCI).*

Munoz-Ramirez, D. O., Reyes-Reyes, R., Ponomaryov, V., & Cruz-Ramos, C. (2015). Invisible digital color watermarking technique in anaglyph 3D images. *2015 12th International Conference on Electrical Engineering, Computing Science and Automatic Control (CCE).*

Dhaou, D., Jabra, S. B., & Zagrouba, E. (2019). A Review on Anaglyph 3D Image and Video Watermarking. *3D Research, 10*(2).

Dhaou, D., Jabra, S. B., & Zagrouba, E. (2019). A Robust Anaglyph 3D Video Watermarking based on Multi-sprite Generation. *Proceedings of the 16th International Joint Conference on E-Business and Telecommunications.*

3D anaglyph image watermarking approach. (2018). *Journal of Al-Qadisiyah for Computer Science and Mathematics, 10*(1).

Raheem, O. A. (2020). Effective Algorithm for Security in Digital Images Using Watermarking. *Journal of Advanced Research in Dynamical and Control Systems, 51*(SP3), 297-304.

Singha, A., & Ullah, M. A. (2019). Transform Domain Digital Watermarking with Multiple Images as Watermarks.

Devi, H. S., & Singh, K. M. (2017). A Novel, Efficient, Robust, and Blind Imperceptible 3D Anaglyph Image Watermarking. *Arabian Journal for Science and Engineering, 42*(8), 3521-3533.

Qureshi, A., Megías, D., & Rifà-Pous, H. (2016). PSUM: Peer-to-peer multimedia content distribution using collusion-resistant fingerprinting. *Journal of Network and Computer Applications, 66,* 180-197.

Megías, D., & Qureshi, A. (2017). Collusion-resistant and privacy-preserving P2P multimedia distribution based on recombined fingerprinting. *Expert Systems with Applications, 71,* 147-172.

Y, R., & Krishna, K. R. (2016). Digital Watermarked Anaglyph 3D Images Using FrFT. *International Journal of Computer Trends and Technology, 41*(2), 77-80.

Bhatnagar, G., Wu, J., & Raman, B. (2010). A robust security framework for 3D images. *Journal of Visualization, 14*(1), 85-93.

Nikolaidis, N., & Pitas, I. (1998). Robust image watermarking in the spatial domain. *Signal Processing, 66*(3), 385-403.

Khan, M. A., Khan, U., & Ali, A. (2018). Chaos Based Spatial Domain Robust Image Watermarking Scheme. *2018 4th International Conference on Computer and Information Sciences (ICCOINS).*

A Robust Image Watermarking Scheme Based on SVD in the Spatial Domain. (2017). *Future Internet, 9*(3), 45.

Su, Q., & Chen, B. (2017). Robust color image watermarking technique in the spatial domain. *Soft Computing, 22*(1), 91-106.

Yuan, Z., Su, Q., Liu, D., Zhang, X., & Yao, T. (2020). Fast and robust image watermarking method in the spatial domain. *IET Image Processing, 14*(15), 3829-3838.

Adwan, O. (2019). Robust Image Watermarking Method using Wavelet Transform. *Signal & Image Processing an International Journal, 10*(5), 29-38.

Ernawan, F., & Kabir, M. N. (2018). A Robust Image Watermarking Technique with an Optimal DCT-Psychovisual Threshold. *IEEE Access, 6*, 20464-20480.

Singh, A. K., Kumar, B., Singh, S. K., Ghrera, S., & Mohan, A. (2018). Multiple watermarking techniques for securing online social network contents using Back Propagation Neural Network. *Future Generation Computer Systems, 86*, 926-939.

Singh, A. K. (2016). An improved hybrid algorithm for robust and imperceptible multiple watermarking using digital images. *Multimedia Tools and Applications, 76*(6), 8881-8900.

Usha, D., & Rakesh, Y. (2014). Generation of digital watermarked Anaglyph 3D image using DWT. SSRG International Journal of Electronics and Communication Engineering (SSRG-IJECE), 1(7), 33–37.

Patel, R., & Parth, B. (2015). Robust watermarking for Anaglyph 3D images using DWT techniques. International Journal of Engineering and Technical Research, 3(6), 55–58.

Koley, S. (2020). Hardware Implementation of a Fast 3D Anaglyph Image Watermarking Framework for Integration in Consumer Electronics Devices. *2020 Zooming Innovation in Consumer Technologies Conference (ZINC)*.

Deng, H., Chen, L., Zhang, J., & Wang, R. (2012). A 3D Model-Watermarking Algorithm Resistant to Affine Transformation. *2012 Fourth International Conference on Multimedia Information Networking and Security*. 14(1); 85-93.

Prathap, I., & Anitha, R. (2014). Robust and blind watermarking scheme for three-dimensional anaglyph images. *Computers & Electrical Engineering, 40*(1), 51-58.

Dhaou, D., Jabra, S. B., & Zagrouba, E. (2018). An Efficient Group of Pictures Decomposition based Watermarking for Anaglyph 3D Video. *Proceedings of the 13th International Joint Conference on Computer Vision, Imaging and Computer Graphics Theory and Applications*.

Devi, H. S., & Singh, K. M. (2016). A robust and optimized 3D red-cyan anaglyph blind image watermarking in the DWT domain. *Contemporary Engineering Sciences, 9*, 1575-1589.

Kahlessenane, F., Khaldi, A., Kafi, R., & Euschi, S. (2021). A robust blind medical image watermarking approach for telemedicine applications. *Cluster Computing*.

Cheema, A. M., Adnan, S. M., & Mehmood, Z. (2020). A Novel Optimized Semi-Blind Scheme for Color Image Watermarking. *IEEE Access, 8*, 169525-169547.

Murty.p, S., R, H. B., & Kumar.p, R. (2012). A Novel Semi-Blind Reference Color Image Watermarking using DWT-DCT-SVD. *International Journal of Computer Applications, 53*(15), 22-28.

Abodena, O., & Agoyi, M. (2018). Color Image Blind Watermarking Scheme Based on Fast Walsh Hadamard Transform and Hessenberg Decomposition. *Studies in Informatics and Control, 27*(3), 339-348.

Dhar, P. K., Chowdhury, A. H., & Koshiba, T. (2020). Blind Audio Watermarking Based on Parametric Slant-Hadamard Transform and Hessenberg Decomposition. *Symmetry*, *12*(3), 333.

ABODENA, O. & AGOYİ, M. (2016). The Color Image Watermarking Algorithm Based on Hessenberg Decomposition. (2016). *Color Image Watermarking*, 155-167.

Su, Q. (2016). Novel blind color image-watermarking technique using Hessenberg decomposition. *IET Image Processing*, *10*(11), 817-829.

Islam, R., & Kim, J. (2014). Reliable RGB color image watermarking using DWT and SVD. *2014 International Conference on Informatics, Electronics & Vision (ICIEV)*.

Babu, S. G., & Ilango, B. S. (2018). Digital Color Image Watermarking Using DWT SVD Cuckoo Search Optimization. *Bio-Inspired Computing for Image and Video Processing*, 227-243.

Kuraparthi, S., Kollati, M., & Kora, P. (2019). Robust Optimized Discrete Wavelet Transform-Singular Value Decomposition Based Video Watermarking. *Traitement Du Signal*, *36*(6), 565-573.

Nandi, S., & Santhi, V. (2018). Digital Image Watermarking Scheme in Transform Domain Using the Particle Swarm Optimization Technique. *Bio-Inspired Computing for Image and Video Processing*, 245-263

Takore, T. T. (2017). An Improved Digital Image Watermarking Scheme using Particle Swarm Optimization Technique. *International Journal for Research in Applied Science and Engineering Technology*, *V* (XI), 1391-1403.

Zheng, Z., Saxena, N., Mishra, K., & Sangaiah, A. K. (2018). Guided dynamic particle swarm optimization for optimizing digital image watermarking in industry applications. *Future Generation Computer Systems*, *88*, 92-106.

Zhou, N. R., Luo, A. W., & Zou, W. P. (2018). Secure and robust watermark scheme based on multiple transforms and Particle Swarm Optimization algorithm. *Multimedia Tools and Applications*, *78*(2), 2507-2523.